Journal of Catalysis 279 (2011) 66–74

Contents lists available at ScienceDirect

Journal of Catalysis

journal homepage: www.elsevier.com/locate/jcat

Supported nitrogen-modified Pd nanoparticles for the selective hydrogenation of 1-hexyne

Micaela Crespo-Quesada, Ryan R. Dykeman, Gabor Laurenczy, Paul J. Dyson, Lioubov Kiwi-Minsker *

Institute of Chemical Sciences and Engineering, Ecole Polytechnique Fédérale de Lausanne (EPFL), CH-1015 Lausanne, Switzerland

ARTICLE INFO

Article history:
Received 26 September 2010
Revised 8 December 2010
Accepted 4 January 2011
Available online 15 February 2011

Keywords:
Heterogeneous catalysis
Bipyridine ligands
Catalyst modifier
1-Hexyne hydrogenation
Palladium nanoparticles
Carbon nanofiber
Structured support
Ionic liquid

ABSTRACT

2,2′-Bipyridine (bipy) and an imidazolium-functionalized bipy ligand were used in the synthesis of palladium nanoparticles in water and in ionic liquid. The function of such ligands was twofold: first, as stabilizing agents to prevent the agglomeration of the nanoparticles during synthesis, and second, to act as *permanent catalyst modifiers*. The N-modified Pd nanoparticles were subsequently deposited onto Carbon Nanofiber-based structured supports and tested in the liquid-phase hydrogenation of 1-hexyne. The catalysts were found to be significantly more selective (up to 98.5% at 25% conversion) than a reference catalyst with non-modified Pd nanoparticles on the same support (88%). Moreover, the high selectivity was maintained up to full conversion, and thus, the over-hydrogenation was suppressed due to a site-blocking effect of the N-containing ligands. The imidazolium-functionalized bipy ligand was found to interact more strongly with the nanocarbon support reinforcing Pd anchoring and reducing leaching into the liquid media.

1. Introduction

About 20% of the reactions used to produce fine chemicals and pharmaceuticals are hydrogenations [1]. Supported Pd nanoparticles (NPs) are known to selectively catalyze the hydrogenation of alkynes to alkenes [2]. The yield of the alkene hydrogenation product increases considerably when modifiers are added to the reaction mixture. Recently, DFT calculations have been used to explain the effect of CO, a commonly used modifier for gas-phase hydrogenations, on the activity and selectivity of Pd in the hydrogenation of acetylene [3].

In liquid-phase reactions, common modifiers include nitrogen-containing ligands (ammonia, quinoline [4–7], pyridine, etc.) and sulfur-containing compounds [8]. Phenanthroline and 2,2′-bipyridine (bipy) have also been used to stabilize Pd NPs with the former (including alkylated derivatives) used for various partial hydrogenation reactions in both organic solvents [9,10] and ionic liquids (ILs) [11].

The mechanism responsible for the increase in selectivity in the presence of modifiers is reaction specific, but in general, it can be due to:

- A "ligand" effect – a nucleophilic modifier increases the electron density of the palladium surface through electron donation from the coordinating ligand [4] that leads to a change in the alkyne/alkene relative strength of adsorption. A decrease in alkene heat of adsorption favors its desorption and increases the selectivity [4,12–14].
- Poisoning (site blocking) [8] via preferential adsorption of the modifier compared to the alkene [5].

The molar ratio of nitrogen-containing ligand to substrate used in hydrogenations ranges from 2 to ~1500 [14–17], and the selectivity toward the alkene increases with modifier concentration. Activity, on the other hand, may either decrease or increase depending on the metal dispersion. Indeed, the turnover frequency (TOF) of the liquid-phase hydrogenation of 1-butyne was found to increase by a factor of 5 over highly dispersed catalysts in the presence of piperidine, but this effect was found to be negligible at low dispersions. Piperidine, being an electron-donating ligand, decreases the strong binding energy of alkynes on small metal particles, which increases the activity [14]. Increased activity was also observed for phenylacetylene hydrogenation in the presence of quinoline at high ligand:Pd molar ratios [17]. However, other studies report that a decrease in activity takes place at a base/Pd molar ratio of ~1500 due to site blocking [5].

Additives can be either added to the reaction mixture (*reaction modifiers*) or introduced as a component of the catalyst (*catalyst modifiers*). According to the latter approach, a 0.5% Pd/Al_2O_3 catalyst treated with Zn acetate, pyridine, and KOH showed high selectivity (up to 99.8%) in 2-methyl-3-butyn-2-ol hydrogenation in

* Corresponding author. Address: EPFL-SB-ISIC-GGRC, Station 6, Switzerland. Fax: +41 21 693 31 90.
E-mail address: lioubov.kiwi-minsker@epfl.ch (L. Kiwi-Minsker).

0021-9517/$ - see front matter © 2011 Elsevier Inc. All rights reserved.
doi:10.1016/j.jcat.2011.01.003

Nomenclature

[BIHB]Br_2 {4,4′-bis[7-(2,3-dimethylimidazolium)heptyl]-2,2′-bipyridine}bromide
[bmim][PF_6] 1-butyl-3-methyl-imidazolium hexafluorophosphate
[C_2OHmim][BF_4] 1-(2-hydroxyethyl)-3-methyl-imidazolium tetrafluoroborate
[C_3CNmim][Tf_2N] 1-(3-cyanopropyl)-3-methyl-imidazolium bis(trifluoromethane)sulfonimide
Bipy 2,2′-bipyridine
CNF carbon nanofiber
SMF sintered metal filter
SC supported catalyst

Symbols

C_i	concentration of a given species, i [mol L^{-1}]
D	dispersion of a nanoparticle [%]
k_i	apparent kinetic constant of the reaction i [L mol_{Pd}^{-1} s^{-1}]
K_i	adsorption constant of i [L mol^{-1}]
m_{Pd}	amount of active material in the catalyst [mol]
r_i	rate of the reaction i [mol mol_{Pd}^{-1} s^{-1}]
V	volume of liquid in the reaction [L]
X	conversion of 1-hexyne [%]

ethanol at a reduced hydrogen pressure [13]. A permanent modification of Pd NPs with pyridine has been achieved by stabilizing them inside poly-4-vinylpyridine block-copolymers – either polystyrene-block-poly-4-vinylpyridine [18,19] or poly(ethylene oxide) – block-poly-2-vinylpyridine [20]. Both systems were studied in the hydrogenation of dehydrolinalool and showed 99% selectivity, which was attributed to the electronic effects of the pyridine functionality on the Pd surface. It has been noted that functionalized phenanthroline stabilizers, for example, substituted with sulfonate groups, can result in problems associated with the immobilization of the resulting NPs. However, alkyl chains in the 3-position have been shown to decrease isomerization during the partial hydrogenation of 2-hexyne [9,21]. Furthermore, bipy and a dipyridyl amine functionalized with an imidazolium moiety have been used to stabilize Rh and Pd NPs that effectively catalyzed the hydrogenation of arenes and alkenes, respectively [22–24].

Sintered Metal Fibers (SMF) with a porosity of 80%, high mechanical strength, and effective heat transfer properties are advantageous structured supports. In order to increase the low specific surface area of the SMFs, carbon nanofibers (CNF) were grown on the surface, thus providing a tridimensional mesoporous chemically inert graphite-like structure [25,26]. This composite support can be subsequently oxidized to generate surface oxygen-containing groups, thus enabling an active phase to be strongly anchored.

In the studies reported herein, an in-house-synthesized imidazolium-tagged bipy ligand and bipy itself were used in the synthesis of monodispersed Pd NPs with a dual aim: stabilizing the nanoparticles by anchoring them to the support and inducing a permanent modification of the surface. To the best of our knowledge, the combination of a functionalized structured support and a tailor-made ligand capable of strongly interacting in order to minimize leaching while increasing selectivity has not been previously reported. The resulting catalysts were tested in the liquid-phase hydrogenation of 1-hexyne in *n*-heptane, and their performance was compared to that of a reference Pd/CNF/SMF catalyst, prepared by a conventional ion-exchange method [25] in the absence of modifiers. The catalysts were further characterized by scanning and transmission electron microscopy (SEM and TEM), X-ray photoelectron spectroscopy (XPS), and CO-chemisorption in order to rationalize the catalytic response observed.

2. Materials and methods

2.1. Materials

All chemicals were purchased from commercial sources and used without further purification. All manipulations were performed in air unless otherwise specified. Reactions performed under N_2 were carried out using standard Schlenk-line techniques or in a dry-box. Toluene was dried catalytically under nitrogen using a solvent purification system manufactured by Innovative Technology Inc, and water was purified with a Pure Water System supplied by PG-Instruments. 4,4′-Bis(7-bromoheptyl)-2,2′-bipyridine [27], [bmim][PF_6] [28], [C_2OHmim][BF_4] [29], and [C_3CNmim][Tf_2N] [30] were synthesized according to literature procedures.

2.2. Preparation of the Pd/CNF/SMF reference catalyst

Synthesis of the composite CNF/SMF support is detailed elsewhere [26]. Briefly, after a calcination step of the $SMF_{Inconel}$ to increase surface roughness followed by a reduction step, ethane decomposition in the presence of hydrogen is performed at 655 °C for 1 h rendering the SMFs homogeneously coated by a CNF layer (~1 μm). The composites were then treated in boiling hydrogen peroxide for 4 h in order to generate oxygen-containing groups on the surface of the CNFs.

The method used to synthesize and immobilize the Pd NPs onto the supports has been reported elsewhere [25]. Briefly, the activated CNF/SMF supports were immersed in a solution containing a Pd precursor (Na_2PdCl_4) for 5 h at room temperature. Afterward, they were dried, calcined, and reduced for 18 h, thus generating Pd NPs with a mean diameter of ~6.7 nm.

2.3. N-modified Pd catalyst preparation

2.3.1. N-containing ligand synthesis

{4,4′-Bis[7-(2,3-dimethylimidazolium)heptyl]-2,2′-bipyridine}bromide ([BIHB]Br_2). Under an atmosphere of nitrogen, 4,4′-bis(7-bromoheptyl)-2,2′-bipyridine (0.638 g, 1.25 mmol) and 1,2-dimethylimidazole (0.804 g, 8.54 mmol) in toluene (50 mL) were stirred under reflux for 20 h, after which a white solid formed. The solid was removed by filtration and washed with ether (20 mL), and residual solvent was removed *in vacuo* to give [BIHB]Br_2 (0.829 g, 94%) (see Scheme 1). Anal. Calc. for $C_{34}H_{50}Br_2N_6$: C, 58.12%; H, 7.17%; N, 11.96%. Found: C, 58.18%; H, 7.45%; N, 11.86%. ^{1}H NMR (400 MHz, D_2O): δ = 8.33 (d, J = 4.9 Hz, 2H), 7.73 (s, 2H), 7.22 (m, 2H+2H), 7.11 (d, J = 4.4 Hz, 2H), 3.93 (t, J = 7.3 Hz, 4H), 3.67 (s, 6H), 2.46 (m, 4H+6H), 1.61 (m, 4H), 1.59 (m, 4H), 1.41, 1.11 ppm (M, 12H). ^{13}C NMR (400 MHz, D_2O): d = 154.80, 154.32, 148.76, 143.95, 124.72, 122.15, 121.76, 120.61, 48.07, 34.64, 29.49, 28.94, 28.17, 28.11, 25.48, 8.93 ppm.

2.3.2. Pd nanoparticle synthesis and immobilization

Both bipy and [BIHB]Br_2-stabilized Pd NPs were prepared using the same procedure. In a typical experiment, $Pd(CH_3CO_2)_2$ (5.6 mg,

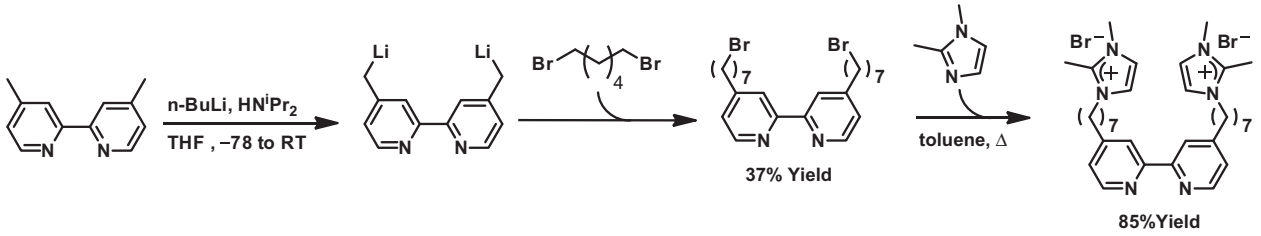

Scheme 1. Synthetic route for the modified bipyridine stabilizer, [BIHB]Br_2.

0.025 mmol), bipy (3.9 mg, 0.025 mmol) in 4 mL of either water or [bmim][PF_6] were stirred for 10 min and then placed in an ultrasonic bath for a further 10 min. The mixture was then placed in an autoclave, pressurized to 10 bar under H_2, and stirred for 1 h. The reduction resulted in an opaque black solution, which was then stirred for 1 h while exposed to air.

The Pd NPs obtained were separated by centrifugation, suspended in fresh solvent, separated again by centrifugation, and then redispersed in acetone. The nanoparticles were subsequently deposited onto the activated CNF/SMF supports (see above) by incipient wetness impregnation and dried for 15 h at 50 °C under vacuum.

2.4. Hydrogenation reactions

Hydrogenations were carried out in a semi-batch stainless steel reactor (250 mL autoclave, Büchi AG, Switzerland) equipped with a heating jacket and a hydrogen supply system. The structured catalyst was placed between two metal gauzes (2 × 8.5 cm) fixed on a self-gassing hollow shaft, which was used as the stirrer. The reactor was charged with 1-hexyne (4.13 g) and octane (2.82 g) and filled to 200 mL with *n*-heptane. The reactor was flushed with N_2 and set to the target temperature. The reactor was then flushed with H_2 and pressurized. The consumption of hydrogen was monitored using a Pressflow gas Controller (BPC-6002) (Büchi, Switzerland).

In addition, samples were periodically withdrawn from the reactor via a sampling tube and analyzed by GC. GC analysis was performed using an Auto System XL (Perkin Elmer) equipped with a 100 m Petrocol DH 0.25 mm capillary column with a 0.5 μ coating at an oven temperature of 333 K. The pressure of the carrier gas (He) was 280 kPa. The temperature of the Injector and the FID was 493 K, and *n*-octane was used as internal standard.

The conversion and selectivity were calculated from:

$$X_{1-hexyne} = \frac{C^0_{1-hexyne} - C_{1-hexyne}}{C^0_{1-hexyne}} \quad (1)$$

$$S = \frac{C_i}{\sum_{products} C_i} \cdot 100 \quad (2)$$

The turnover frequency (TOF) was calculated as:

$$TOF_g\ [s^{-1}] = \frac{r\ [\mathrm{mol/mol_{Pd}\ s}]}{D} \quad (3)$$

where *D* is the dispersion of the nanoparticle, defined as the ratio between the number of surface atoms and the total number of atoms of the nanoparticle, and *r* is the measured transformation rate expressed in mols of 1-hexyne consumed per mol of Pd and per unit of time.

For the leaching experiments, the catalysts were placed in the stirrer cage and subjected to the same conditions as the reaction runs except for hexyne in the liquid phase.

2.5. Characterization techniques

NMR spectra were recorded on either an Avance 400 MHz or a 400 MHz Bruker DRX instrument with ^{1}H chemical shifts referenced to residual solvent peaks.

X-ray photoelectron spectroscopy (XPS) data were collected by an Axis Ultra instrument (Kratos analytical, Manchester, UK) under ultra-high-vacuum condition (<10^{-8} Torr) and using a monochromatic Al Kα X-ray source (1486.6 eV). The source power was maintained at 150 W, and the emitted photoelectrons were sampled from a square area of 750 × 350 μm^2. The photoelectron take-off angle, between the surface and the direction in which the photoelectrons were analyzed, was 90°. The analyzer pass energy was 80 eV for survey spectra (0–1000 eV) and 40 eV for high-resolution spectra: Pd $3d_{5/2}$, O 1s, and C 1s. The adventitious carbon 1s peak was calibrated at 284.5 eV and used as an internal standard to compensate for any charging effects. Both curve fitting of the spectra and quantification were performed with the CasaXPS software, using relative sensitivity factors given by Kratos.

To determine the amount of Pd in the catalyst, the catalyst was dissolved in hot nitric acid, and the sample was analyzed by atomic absorption spectroscopy via Shimadzu AA-6650 spectrometer with an air–acetylene flame.

Pd dispersion was measured by pulse adsorption of CO (3% CO in He) carried out at 323 K in a Micromeritics AutoChem 2910. Before measurements, the catalyst was pretreated at 353 K in flows of He (10 mL/min, STP), H_2 (20 mL/min, STP), and He (10 mL/min, STP). A stoichiometry of CO/Pd = 0.6 and a Pd surface density of 1.2 × 10^{19} atoms/m^2 were used for these calculations.

TEM pictures were obtained using a Philips CM20 Electron Microscope operating at 200 kV. SEM images were recorded on a FEI XL-30 SFEG Sirion Electron Microscope equipped with a TLD detector.

The solubility of H_2 in [C_3CNmim][Tf_2N] was estimated using a literature method [31]. At a pressure of 100 atm H_2, 2.5 mL of the IL was sealed in a sapphire NMR tube. After vigorous shaking, a ^{1}H NMR spectrum of the solution was recorded. The ^{1}H NMR spectrum was fitted with WINNMR and NMRICMA2.8/MATALAB programs (nonlinear least squares fit, minimizing the difference between the measured and calculated spectra to determine the spectral parameters and integrals). The Henry's constant for H_2 was found to be 510 MPa and the hydrogen concentration 1.28 mM at 1 atm [32].

In order to measure solubility of the organic compounds in the ILs, an excess of the compound (either *n*-hexane, 1-hexene or 1-hexyne) was added to a 3-mL screw cap vial containing a magnetic stir bar and the IL ([bmim][PF_6], [C_2OHmim][BF_4] or [C_3CNmim][Tf_2N]) and mixed at room temperature (20.0 °C) for 14 h, after which time the majority of the IL and a fraction of the organic compound were transferred to a 5-mm NMR tube and allowed to settle to ensure only the IL layer would be analyzed by the receiver coil. Spectra were recorded at 25.1 °C without an internal reference. The resulting ^{1}H NMR spectra were analyzed using Bruker TOPSPIN 1.3 NMR software with deconvolution (fit type

of Lorentzian) employed where necessary to obtain the appropriate integration.

3. Results and discussion

3.1. Catalysts used in this work

Table 1 lists the catalysts used throughout this work and provides a succinct description of the procedure used for their synthesis; for more detailed descriptions see Sections 2.2 and 2.3.

3.2. Hydrogenation of 1-hexyne over the reference Pd/CNF/SMF catalyst

The morphology of the reference catalyst comprises a network of CNFs with an individual diameter of approximately 40–50 nm coating the surface of each fiber (of approximately 8 μm in diameter) of the $SMF_{Inconel}$ (Fig. 1a). The white dots that can be observed in the SEM image are Ni particles that are detached from the SMF during the formation of the CNF and serve as catalysts for the formation of the latter, as confirmed by EDX [26]. The TEM image presented in Fig. 1b shows monodispersed (~7 nm) Pd NPs that are evenly distributed along a single CNF. The mean particle size was also estimated via CO-chemisorption, yielding a value of 6.7 nm, in good agreement with the TEM images. Fig. 1c shows a TEM image of an isolated CNF. It can be appreciated that the Ni particle at the tip of the fiber is covered by several layers of graphitic carbon. The inset of the image shows a high resolution image of the graphite-coated Ni nanoparticle. This layer of graphite ensures their inertness.

Before comparing catalyst performances or deriving kinetic expressions, it is necessary to verify whether the system operates under kinetic regime. Both heat and internal and external mass transfer influences were assessed for the reference catalyst. The detailed discussion can be found in the Supporting Information. Under the conditions used, the reaction was found to be under the kinetic regime for the reference catalyst; being the most active catalyst studied, this ensures a similar result for all the others.

The reference catalyst showed a high activity in the hydrogenation of 1-hexyne with a TOF ~200 s^{-1} (see Scheme 2 for the reaction network). The formation of *n*-hexane takes place not only in a consecutive (path 2, Scheme 2) but also in a parallel way (path 3, Scheme 2) since their formation is already detected at conversions close to zero. 2-hexene isomers were almost undetectable until the maximum yield of 1-hexene was reached. After the complete

Table 1
Catalysts used during this work.

Catalyst	Stabilizer	NP synthesis in	IL coating	% Pd[a]	% IL
Reference	–	–	–	0.6[b]	–
Reference	–	–	[bmim][PF_6]	0.82[b]	4.2
Reference	–	–	[C_2OHmim][BF_4]	0.48[b]	5.4
Reference	–	–	[C_2CNmim][Tf_2N]	0.62[b]	4.2
SILC(Bip)	Bipy	[bmim][PF_6]	[bmim][PF_6]	4.0	3.0
SILC(Bih)	[BIHB]Br_2	[bmim][PF_6]	[bmim][PF_6]	3.9	3.7
SC(Bip)	Bipy	H_2O	–	3.2	–
SC(Bih)	[BIHB]Br_2	H_2O	–	2.0	–

[a] Percentage expressed per mass of CNFs.
[b] Percentage expressed per total mass of the catalyst.

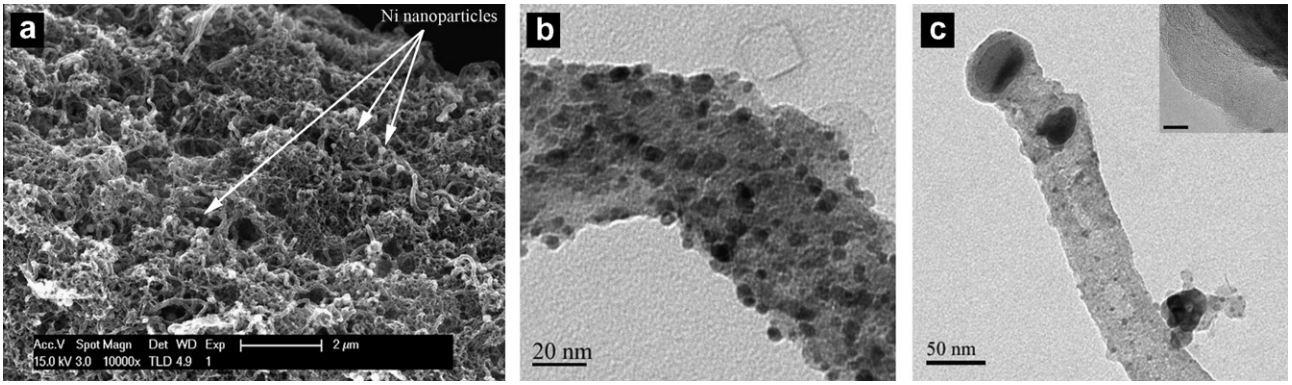

Fig. 1. Morphology of the reference catalyst. (a) SEM image of the CNF/SMF support and (b) TEM showing well-dispersed Pd NPs anchored onto the CNF (c) TEM of a single CNF where the graphitic layer protecting the Ni particle can be appreciated. The inset shows a HR-TEM image of the nanoparticle where the layers of C can be seen. The scale bar in the inset corresponds to 10 nm.

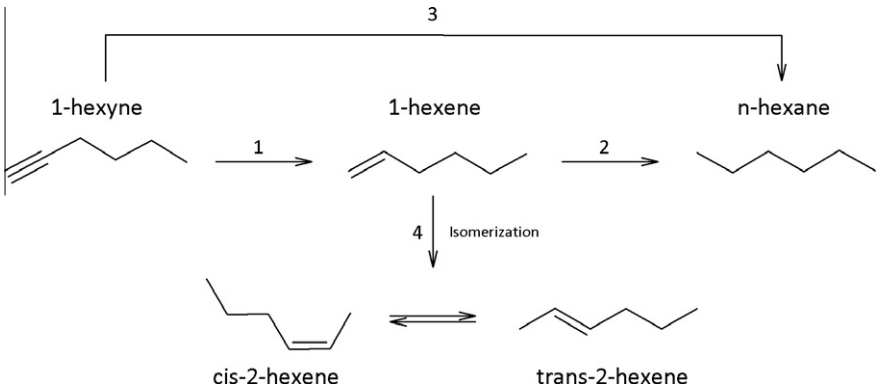

Scheme 2. Reaction network for the hydrogenation of 1-hexyne.

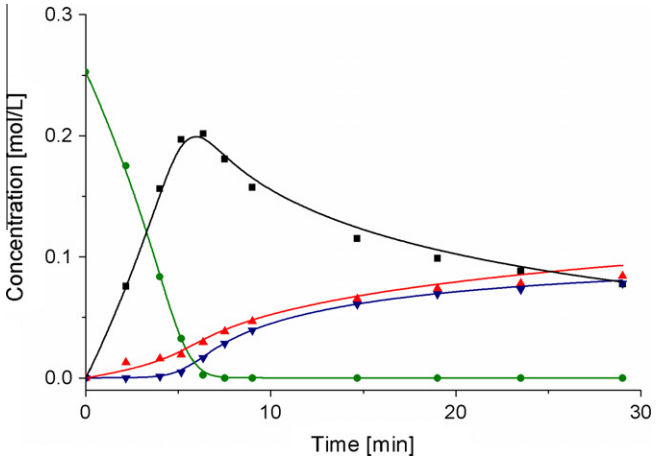

Fig. 2. Experimental points and kinetic curves modeled using Berkeley's Madonna software for the reference catalyst. ● 1-Hexyne, ■ 1-hexene, ▲ *n*-hexane, ▼ 2-hexene isomers. Reaction conditions: 4.1 g of 1-hexyne, 2.82 g of octane as internal standard, 0.3 g of catalyst, 303 K, and 1.05 MPa of H_2 in 200 mL of *n*-heptane.

consumption of 1-hexyne, 1-hexene was rapidly transformed into hexane and its two isomers with a ratio of 1:1 (Fig. 2).

A Langmuir–Hinshelwood mechanism was applied for modeling the kinetics assuming dissociative weak adsorption of hydrogen. For path 1 and 3 (Scheme 2), the second addition of hydrogen was considered as the rate-determining step. For path 2, the first addition of hydrogen was considered as the rate-determining step. The adsorption equilibrium constants of the hydrogenated products are small compared to the initial acetylenic compound. Therefore, the adsorption constants of *n*-hexane and the alkene isomers, *K*, were considered to be equal. This assumption, together with the weak hydrogen adsorption on Pt group metals [33], allows the following (simplified) equations to be deduced (see the list of symbols, subscripts Y, E, A, and I refer to the alkyne, alkene, alkane, and isomers, respectively):

$$r_1 = \frac{k_1 K_Y C_Y K_H C_H}{(1 + K_Y C_Y + K_E C_E + K(C_A + C_I))^2} \tag{4}$$

$$r_2 = \frac{k_2 K_Y C_Y K_H C_H}{(1 + K_Y C_Y + K_E C_E + K(C_A + C_I))^2} \tag{5}$$

$$r_3 = \frac{k_3 K_Y C_Y K_H C_H}{(1 + K_Y C_Y + K_E C_E + K(C_A + C_I))^2} \tag{6}$$

$$r_4 = \frac{k_4 K_E C_E^2}{(1 + K_Y C_Y + K_E C_E + K(C_A + C_I))^2} \tag{7}$$

In order to ascertain an overall kinetic rate equation, the full set of differential equations describing the concentration variation of all species participating in the reaction is required (subscripts 1, 2, 3, and 4 refer to the different reaction paths in Scheme 2):

$$\frac{dC_Y}{dt} = (-r_1 - r_3) \tag{8}$$

$$\frac{dC_E}{dt} = (r_1 - r_2 - r_4) \tag{9}$$

$$\frac{dC_A}{dt} = (r_2 + r_3) \tag{10}$$

$$\frac{dC_I}{dt} = r_4 \tag{11}$$

Table 2
Adsorption and kinetic constants found for the reference catalyst and SILC(Bih).[a]

Adsorption constants ($L\ mol^{-1}$)			Kinetic constants ($mol\ g_{Pd}^{-1}\ s^{-1}$)		
	Reference	SILC(Bih)		Reference	SILC(Bih)
K_Y	23.1	35.9	k_1	2486.1	2503.3
K_N[b]	–	9.6	k_2	1162.3	54.1
K_E	0.8	0.1	k_3	208.8	154.4
K	8.3	4.7	k_4	11.1	10.1
K_H[c]	1×10^{-3}	2×10^{-3}			

[a] Reaction conditions: 4.1 g of 1-hexyne, 2.82 g of octane as internal standard, 0.3 g of catalyst, 303 K, and 1.05 MPa of H_2 in 200 mL of *n*-heptane.
[b] Dimensionless.
[c] This constant is the product $K_{H_2} C_{H_2}$ and is dimensionless.

These eight Eqs. (4)–(11) can be solved simultaneously using Berkeley's Madonna software [34] with Rosenbrock's method [35]. The model parameters were estimated by fitting the simulated curves to the experimental data giving the kinetic constants k_1–k_4 and the adsorption constants K_Y, K_E, K_H, and K presented in Table 2. It is worth noting that fitting such expressions makes the result dependent on the starting values given to the constants. In order to obtain reliable results, the starting values for each constant are set and certain constraints applied, such as hydrogen adsorption constant much smaller than the rest, no negative values and higher values for k_1 and K_Y. This kinetic model has been successfully applied for other liquid-phase alkyne hydrogenations over palladium catalysts [36,37]. Fig. 2 shows the prediction curves obtained with the kinetic model proposed. A correlation coefficient of 98.5% was achieved according to Eq. (12).

$$r^2 = \left[\frac{\Sigma(x - \bar{x})(y - \bar{y})}{\sqrt{\Sigma(x - \bar{x})^2 \Sigma(y - \bar{y})^2}} \right]^2 \tag{12}$$

The adsorption constant of 1-hexyne was found to be 2 orders of magnitude higher than that of 1-hexene, in line with other results reported for hydrogenations over Pd [37,38]. Furthermore, the adsorption constant of hydrogen was 5 orders of magnitude smaller than that of the alkyne, thus validating the weak adsorption assumption made when developing the model. The kinetic constant of the first reaction (path 1, Scheme 2) was only twice as high as that for the over-hydrogenation (path 2, Scheme 2). This is in agreement with the thermodynamic basis for the selectivity proposed by Molnar et al. [12], i.e., the high selectivity toward the alkene is due to a stronger adsorption of the alkyne, compared to the alkene, rather than a higher kinetic constant of different hydrogenation steps.

3.3. Hydrogenation of 1-hexyne over the N-modified Pd catalysts

3.3.1. N-modified Pd NPs

Fig. 3 shows TEM images and the particle size distributions of each sample of the bipy-stabilized Pd NPs synthesized in water and in [bmim][PF_6]. The solvent influences the mean diameter of the NPs, but the ligand (either bipy or [BIHB]Br_2) does not, with approximately the same particle size distribution in the two solvents independent of the ligand employed. Pd loading on CNFs was found to be between 2% and 4%.

3.3.2. Catalytic effect of N-containing ligands: supported N-modified Pd NPs synthesized in [bmim][PF_6]

Fig. 4 shows the catalytic results for SILC(Bih) (see Table 1) in the hydrogenation of 1-hexyne. The differences compared to the reference catalyst (Fig. 2) are significant, since the over-hydrogenation toward the alkane (path 2, Scheme 2) appears to be

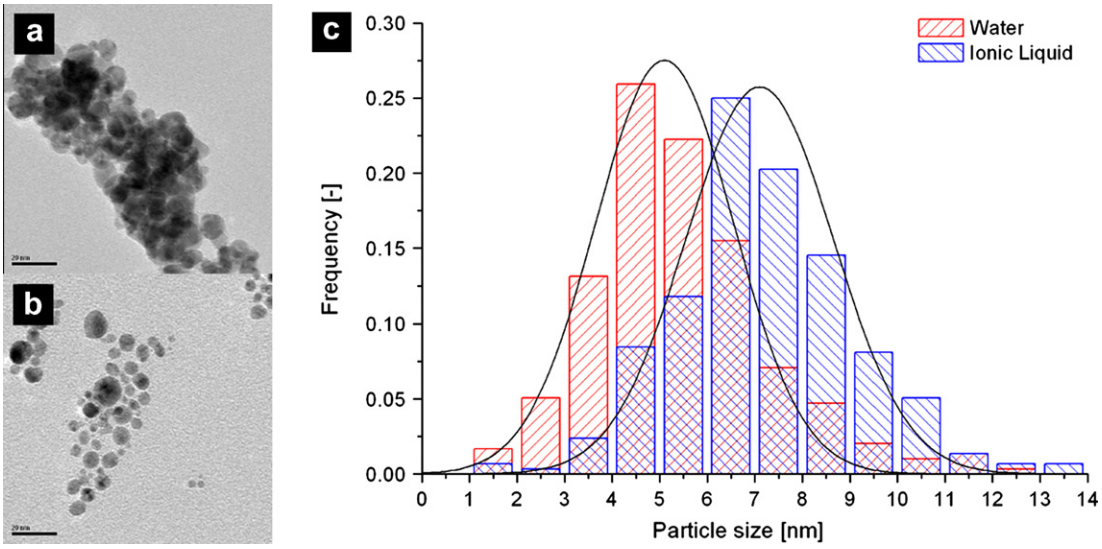

Fig. 3. TEM images and (c) particle size distribution of the Pd NPs synthesized with bipy as stabilizer in (a) [bmim][PF_6] and (b) water.

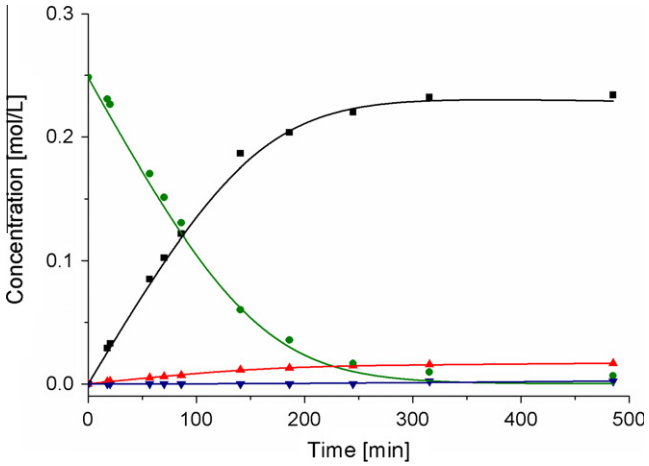

Fig. 4. Experimental points and kinetic curves modeled using Berkeley's Madonna software for SILC(Bih). ● 1-Hexyne, ■ 1-hexene, ▲ *n*-hexane, ▼ 2-hexene isomers. Reaction conditions: 4.1 g of 1-hexyne, 2.82 g of octane as internal standard, 0.3 g of catalyst, 303 K, and 1.05 MPa of H_2 in 200 mL of *n*-heptane.

completely suppressed. Furthermore, both the initial selectivity and the maximum yield of 1-hexene increased by 10%. A similar effect, albeit less pronounced, was observed with a *S*-based modifier [36] and quinoline [37] added to the reaction mixture in the liquid-phase hydrogenation of 2-methyl-3-butyn-2-ol.

The same kinetic model as described above was used with the exception that a new dimensionless constant, K_N, was added in the denominator of Eqs. (4)–(7) to take into account the permanent adsorption of the N-containing ligands on the Pd NP surface:

$$r_1 = \frac{k_1 K_Y C_Y K_H C_H}{((1 + K_N) + K_Y C_Y + K_E C_E + K(C_A + C_I))^2} \quad (13)$$

A comparison of the constants is provided in Table 2. The results shown suggest two possible explanations for the effect of the N-containing ligands.

First, the initial coverage of the modifier ($\theta_N = 0.49$) is slightly higher than the maximum coverage of the substrate ($\theta_Y = 0.46$) and is 2 orders of magnitude higher than the maximum coverage of the desired product ($\theta_E = 2.4 \times 10^{-3}$). In order to determine whether the alkyne and the modifier were in a dynamic adsorption/desorption regime, 0.2 g of the catalyst was stirred in 200 mL of heptane containing 4.1 g of hexyne at 30 °C for 3 h. The sample was studied by ^{1}H NMR spectroscopy, and both bipy and [BIHB]Br_2 were below the detection limit. The concentration may be thus estimated to be <3.75 μmol/L. This implies that in order to react, the alkyne must temporarily displace the modifier from the active site, which probably adopts a more packed adsorption conformation, which is reverted to the original mode of adsorption once the alkyne has reacted. Therefore, the N-based ligands most probably increase the selectivity through a permanent site-blocking effect.

Second, an electronic effect is also observed. As suggested in the literature, a nucleophilic ligand increases the electron density of Pd, thus leading to a change in the alkyne/alkene relative strength of adsorption as well as a decrease in alkene heat of adsorption, both of which were observed in the model (Table 2) [4,12–14].

A well-known example of Pd permanent modification aimed at enhancing the selectivity is the addition of Pb to Pd in Lindlar's industrial catalyst [39,40]. In order to compare its effectiveness with the catalytic results reported herein, Lindlar's catalyst (5%Pd 3.5%Pb/$CaCO_3$) was tested under the same reaction conditions (see Supporting Information for details). The selectivity was found to be only 95% at 25% conversion (against 98.5% over our catalyst), but dropped quickly when approaching full conversion. The most important difference is that the over-hydrogenation reaction was not hindered with Lindlar's catalyst, implying that a reaction modifier would have to be added to the reacting mixture in practical use.

3.3.2.1. Catalytic effect of ionic liquids. Supported Pd NPs embedded in ILs have already been found useful for tailoring the selectivity in several liquid-phase hydrogenations [41,42]. ILs exert an electronic effect on embedded Pd NPs in the hydrogenation of acetylene causing an increase in the selectivity toward ethylene [43]. In order to study the effect due solely to the IL in which the NPs were embedded, the reference catalyst was covered with a layer of either [bmim][PF_6], [C_2OHmim][BF_4] or [C_3CNmim][Tf_2N] and tested in the hydrogenation of 1-hexyne.

All catalysts were less active than the reference, and surprisingly, the selectivity toward the target product did not improve significantly. Nevertheless, the product distribution was affected by the type of IL as seen in Fig. 5. With the use of [bmim][PF_6], selectivity toward 2-hexene isomers, particularly the trans-isomer, was increased at the expense of the alkene compared to the

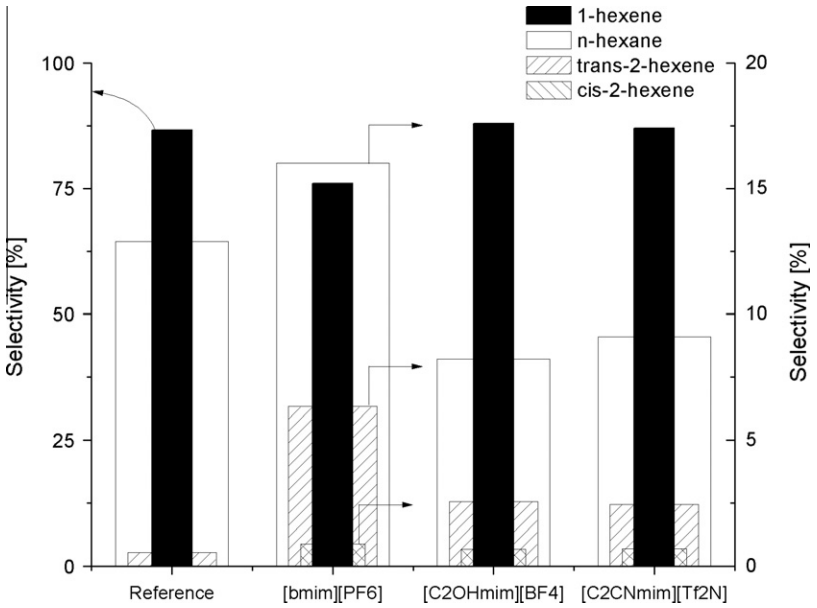

Fig. 5. Product distribution at 50% conversion for the IL-coated reference catalysts. Reaction conditions: 4.1 g of 1-hexyne, 2.82 g of octane as internal standard, 0.3 g of catalyst, 303 K, and 1.05 MPa of H_2 in 200 mL of *n*-heptane.

reference catalyst. Employing either $[C_2OHmim][BF_4]$ or $[C_3CNmim][Tf_2N]$, on the other hand, showed an alkane:isomers ratio significantly lower than that of the reference catalyst. ^1H NMR spectroscopy measurements revealed that the solubility of 1-hexyne, 1-hexene, and *n*-hexane is practically the same in $[bmim][PF_6]$ and $[C_3CNmim][Tf_2N]$ (see Table 4), hence eliminating differences in solubility as being responsible for the differences observed in the product distribution. Differences in H_2 solubility in ILs could also offer a possible explanation [41], but gas solubility measurements showed no correlation between the two (Table 4). A ligand site-blocking effect appears to be the most plausible explanation for the change in product distribution since both hydroxyl and nitrile functionalities can conceivably interact with the Pd surface, as is proposed for Pd NPs prepared in $[C_2OHmim][BF_4]$ and $[C_3CNmim][Tf_2N]$ reactions [30,44,45]. Presumably, coverage of the Pd NP surface by the donor atoms of the IL is very high and influences the reaction selectivity.

3.3.3. Catalytic effect of N-containing ligands: supported N-modified Pd NPs prepared in water

The change in the catalytic behavior may be attributed to the N-modified Pd NPs, and to confirm this hypothesis, the NPs were synthesized in water, separated by centrifugation and redispersed in acetone. The solution was then used for impregnating the CNF/SMF composite supports (SC(Bip) and SC(Bih)), and the resulting catalysts were tested under the same reaction conditions (see Table 3).

Table 3
Performance of the various catalysts tested in the hydrogenation of hexyne.[a]

Catalyst	S^b (%)	R (mol mol_{Pd}^{-1} s^{-1})	TOF (s^{-1})
Reference	88.0	47.0	223.8
SILC(Bip)	97.0	4.3	29.5
SILC(Bih)	94.0	11.0	60.8
SC(Bip)	98.4	1.7	11.5
SC(Bih)	97.8	1.4	7.6

[a] Reaction conditions: 4.1 g of 1-hexyne, 2.82 g of octane as internal standard, 0.3 g of catalyst, 303 K, and 1.05 MPa of H_2 in 200 mL of *n*-heptane.
[b] Selectivity toward 1-hexene at 25% conversion.

A similar behavior in the hydrogenation of 1-hexyne was found regardless of the N-containing ligand used for synthesizing the Pd NPs. The N-modified Pd NPs prepared in water demonstrated the same initial selectivity toward 1-hexene (~98%). Moreover, the reaction rate and TOF were in both cases significantly lower than that of the reference catalyst.

XPS measurements show that the Pd NPs present different oxidation states on their surfaces, as seen in Table 5 for Pd $3d_{5/2}$. All three catalysts contain a peak between 335.2 and 335.4 eV, consistent with metallic Pd. The reference catalyst shows a peak corresponding to Pd^{2+} at 337.2 eV, which can be attributed to PdO. The corresponding band of the two N-modified NPs was significantly shifted to higher values (337.9–338.1 eV) corresponding to Pd^{2+} ions coordinated with the N-containing ligands. Note,

Table 4
Determination of 1-hexyne, 2-hexene, *n*-hexane and H_2 solubility in $[bmim][PF_6]$, $[C_2OHmim][BF_4]$ and $[C_3CNmim][Tf_2N]$ by ^1H NMR spectroscopy.

Ionic liquid	Concentration (M)			
	1-Hexyne	1-Hexene	*n*-Hexane	H_2[a] (mM)
$[bmim][PF_6]$	1.24	0.23	0.07	0.97[b]
$[C_3CNmim][Tf_2N]$	0.85	0.18	0.06	0.47
$[C_2OHmim][BF_4]$	0.17	<0.01	0.06	1.28[c]

[a] Measured at 10.1 MPa and adjusted for 0.101 MPa.
[b] From Ref. [32].
[c] From Ref. [29].

Table 5
Binding energies of Pd 3 5/2.

Catalyst	Pd 3d5/2 (eV)		Reference
	Pd(0)	Pd(II)	
Reference	335.4	337.2	
SC(Bip)	335.3	338.1	
SC(Bih)	335.2	337.9	
Pd(0)	335.4		[53]
PdO		337.1	[54]
$PdCl_2$(bipy)		338.1	[55]
$Pd(C_2H_3O_2)_2$		338.8	[56]

$PdCl_2$(bipy) exhibits a binding energy of 338.1 eV. These results show that the electronic properties of metallic Pd were not altered by the presence of the N-containing ligands. However, Pd^{2+} species present on the surface of the catalyst were indeed strongly affected by the complexation of the N-containing ligands. The presence of multiple oxidation states on the surface of catalysts is known to influence their catalytic properties [46]; here, however, the specific role of the N-modified Pd^{2+} species is not clear, but it is probable that these species contribute to the differences between the Pd NP catalysts.

A supplementary effect of the N-modified stabilizers may be due to the change of the surface chemistry of the carbon-based supports. A useful tool to examine the nature of the oxygen groups present on the surface of the CNF is XPS. The differences in binding energy for various bonding states are quite small for electronegative atoms. It is therefore convenient to measure the C1s signal. Carbon atoms differ in their binding energy if they are bonded to an oxygen atom (phenols, ethers, carbonyl groups) or to two oxygen atoms (carboxyl and lactone groups) [47]. Their corresponding signals appear as satellites on the high binding energy side of the main C1s peak, as shown in Fig. S3 in the Supporting Information. The C1s spectra can be resolved into six individual component peaks comprising carbidic carbon (Peak I), graphitic carbon (Peak II), phenolic or ether groups (Peak III), carbonyl groups (Peak IV), carboxyl or ester groups (Peak V), and satellite peaks due to π–π^* transitions in aromatic rings (Peak VI). The corresponding binding energies at which these peaks appear can be found elsewhere [48,49].

A qualitative inspection of the Fig. S3 shows an increase in the number of carboxylic groups and thus of the acidity of the support upon activation. The deposition of the N-modified Pd NPs affects almost exclusively the carboxylic acid groups and suggests a subsequent reduction in the acidity of the support. However, as the vast majority of the surface oxygen groups lay beyond the detection limit of XPS [49], the effect of the addition of N-containing ligands on acidity must be minimal and the overall increase in selectivity is, as expected, due to interactions of the N-containing ligands with the Pd surface.

3.4. Resistance to leaching

Leaching of active Pd species from the support is one of the main causes for deactivation in three-phase hydrogenations [50–52]. To compare the level of leaching between the bipy and $[BIHB]Br_2$ modified catalysts, two halves of the same disk of CNF/SMF support were impregnated with two N-modified NPs. Both were stirred in 200 mL of heptane at 30 °C, 1.05 MPa of H_2, 2000 rpm for 1 h. The analysis of solvent phase revealed that the $[BIHB]Br_2$ (9% leaching) modified catalyst was more stable than the bipy modified system (14% leaching, implying 55% more leaching in the latter), presumably due to a stronger interaction with the oxygenated surface groups present on the CNF. Ionic interactions between surface-bound O^- atoms and the cationic $[BIHB]^{2+}$ ligands are probably responsible for the higher stability of the system.

4. Conclusions

N-modified Pd-nanoparticles immobilized on CNF/SMF supports were synthesized and studied in the selective hydrogenation of 1-hexyne. The catalysts were found to be significantly more selective (up to 98.5% at 25% conversion) than a reference catalyst with non-modified Pd nanoparticles on the same support (88%). Moreover, the high selectivity was maintained up to full conversion.

A Langmuir–Hinshelwood model was found to be consistent with the observed reaction kinetics and showed that the N-contained ligands permanently adsorb on the Pd surface "blocking" the active sites for 1-hexene adsorption. Nonetheless, an electronic effect from the N-coordinated Pd^{2+} species resulting in a change in the adsorption strengths and kinetic constants also contributes to the change in the catalytic performance.

The imidazolium-functionalized bipy ligand was found to largely reduce Pd leaching from the catalyst presumably due to a stronger ionic interaction with the oxygenated surface groups present on the CNF.

Acknowledgments

The Swiss National Science Foundation is acknowledged for financial support. The authors also thank Nicolas Xanthopoulos (EPFL-SB-CIME) for the XPS measurements.

Appendix A. Supplementary data

Supplementary data associated with this article can be found, in the online version, at doi:10.1016/j.jcat.2011.01.003.

References

[1] C.H. Bartholomew, R.J. Farrauto, Fundamentals of Industrial Catalytic Processes, second ed., Wiley-Interscience, Hoboken, NJ, 2006.
[2] H.-U. Blaser, A. Indolese, A. Schnyder, H. Steiner, M. Studer, J. Mol. Catal. A 173 (2001) 3–18.
[3] M. Garcia-Mota, B. Bridier, J. Perez-Ramirez, N. Lopez, J. Catal. 273 (2010) 92–102.
[4] T. Mallat, A. Baiker, Appl. Catal. A 200 (2000) 3–22.
[5] T.A. Nijhuis, G. van Koten, F. Kaptejn, J.A. Moulijn, Catal. Today 79-80 (2003) 315–321.
[6] R. Schlogl, K. Noack, H. Zbinden, A. Reller, Helv. Chim. Acta 70 (1987) 627–679.
[7] J. Yu, J.B. Spencer, Chem. Commun. (1998) 1103–1104.
[8] R. Tschan, M.M. Schubert, A. Baiker, W. Bonrath, H. Lansink-Rotgerink, Catal. Lett. 75 (2001) 31–36.
[9] G. Schmid, S. Emde, V. Maihack, W. Meyer-Zaika, S. Peschel, J. Mol. Catal. A: Chem. 107 (1996) 95–104.
[10] G. Schmid, M. Harms, J.O. Malm, J.O. Bovin, J. Van Ruitenbeck, H.W. Zandbergen, W.T. Fu, J. Am. Chem. Soc. 115 (1993) 2046–2048.
[11] J. Huang, T. Jiang, B.X. Han, H.X. Gao, Y.H. Chang, G.Y. Zhao, W.Z. Wu, Chem. Commun. (2003) 1654–1655.
[12] A. Molnar, A. Sarkany, M. Varga, J. Mol. Catal. A 173 (2001) 185–221.
[13] E.M. Sulman, Russ. Chem. Rev. 63 (1994) 923–936.
[14] J.P. Boitiaux, J. Cosyns, S. Vasudevan, Appl. Catal. 15 (1985) 317–326.
[15] J. Rajaram, A.P.S. Narula, H.P.S. Chawla, S. Dev, Tetrahedron 39 (1983) 2315–2322.
[16] B.E. Green, C.S. Sass, L.T. Germinario, P.S. Wehner, B.L. Gustafson, J. Catal. 140 (1993) 406–417.
[17] M.A. Aramendia, V. Borau, C. Jimenez, J.M. Marinas, M.E. Sempere, F.J. Urbano, Appl. Catal. 63 (1990) 375–389.
[18] L.M. Bronstein, D.M. Chernyshov, I.O. Volkov, M.G. Ezernitskaya, P.M. Valetsky, V.G. Matveeva, E.M. Sulman, J. Catal. 196 (2000) 302–314.
[19] E. Sulman, Y. Bodrova, V. Matveeva, N. Semagina, L. Cerveny, V. Kurtc, L. Bronstein, O. Platonova, P. Valetsky, Appl. Catal. A: Gen. 176 (1999) 75–81.
[20] N. Semagina, A. Bykov, E. Sulman, V. Matveeva, S. Sidorov, L. Dubrovina, P. Valetsky, O. Kiselyova, A. Khokhlov, B. Stein, L. Bronstein, J. Mol. Catal. A 208 (2004) 273–284.
[21] G. Schmid, Chem. Rev. 92 (1992) 1709–1727.
[22] B. Léger, A. Denicourt-Nowicki, H. Olivier-Bourbigou, A. Roucoux, Tetrahedron Lett. 50 (2009) 6531–6533.
[23] Y. Hu, Y.Y. Yu, Z.S. Hou, H. Li, X.G. Zhao, B. Feng, Adv. Synth. Catal. 350 (2008) 2077–2085.
[24] Y. Hu, H.M. Yang, Y.C. Zhang, Z.S. Hou, X.R. Wang, Y.X. Qiao, H. Li, B. Feng, Q.F. Huang, Catal. Commun. 10 (2009) 1903–1907.
[25] P. Tribolet, L. Kiwi-Minsker, Catal. Today 105 (2005) 337–343.
[26] P. Tribolet, L. Kiwi-Minsker, Catal. Today 102–103 (2005) 15–22.
[27] N. Terasaki, T. Akiyama, S. Yamada, Chem. Lett. (2000) 668–669.
[28] J. Dupont, C.S. Consorti, P.A.Z. Suarez, R.F.d. Sousa, Org. Synth. 79 (2004) 236.
[29] X. Yang, N. Yan, Z.F. Fei, R.M. Crespo-Quesada, G. Laurenczy, L. Kiwi-Minsker, Y. Kou, Y.D. Li, P.J. Dyson, Inorg. Chem. 47 (2008) 7444–7446.
[30] Y.G. Cui, I. Biondi, M. Chaubey, X. Yang, Z.F. Fei, R. Scopelliti, C.G. Hartinger, Y.D. Li, C. Chiappe, P.J. Dyson, Phys. Chem. Chem. Phys. 12 (2010) 1834–1841.
[31] D.B. Zhao, Z.F. Fei, R. Scopelliti, P.J. Dyson, Inorg. Chem. 43 (2004) 2197–2205.
[32] P.J. Dyson, G. Laurenczy, C.A. Ohlin, J. Vallance, T. Welton, Chem. Commun. (2003) 2418–2419.

[33] U.K. Singh, M. Albert Vannice, J. Catal. 191 (2000) 165–180.
[34] R.I. Macey, G.F. Oster, Berkeley MadonnaTM (1997–2001) p.
[35] H.H. Rosenbrock, C. Storey, Computational Techniques for Chemical Engineers, Pergamon Press, Oxford, 1966.
[36] M. Crespo-Quesada, M. Grasemann, N. Semagina, A. Renken, L. Kiwi-Minsker, Catal. Today 147 (2009) 247–254.
[37] N. Semagina, M. Grasemann, N. Xanthopoulos, A. Renken, L. Kiwi-Minsker, J. Catal. 251 (2007) 213–222.
[38] A. Bruehwiler, N. Semagina, M. Grasemann, A. Renken, L. Kiwi-Minsker, A. Saaler, H. Lehmann, W. Bonrath, F. Roessler, Ind. Eng. Chem. Res. 47 (2008) 6862–6869.
[39] H. Lindlar, Helv. Chim. Acta XXXV, Fasciculus II (1952) 446–450.
[40] R. Schlogl, K. Noack, H. Zbinden, A. Reller, Helv. Chim. Acta 70 (1987) 627–679.
[41] J.P. Mikkola, P. Virtanen, H. Karhu, T. Salmi, D.Y. Murzin, Green Chem. 8 (2006) 197–205.
[42] J.P.T. Mikkola, P.P. Virtanen, K. Kordas, H. Karhu, T.O. Salmi, Appl. Catal. A – Gen. 328 (2007) 68–76.
[43] M. Ruta, G. Laurenczy, P.J. Dyson, L. Kiwi-Minsker, J. Phys. Chem. C 112 (2008) 17814–17819.
[44] N. Yan, X. Yang, Z.F. Fei, Y.D. Li, Y. Kou, P.J. Dyson, Organometallics 28 (2009) 937–939.
[45] L. Zhou, L. Wang, Synthesis – Stuttgart (2006) 2653–2658.
[46] G.A. Somorjai, Science 227 (1985) 902–908.
[47] H.P. Boehm, Carbon 40 (2002) 145–149.
[48] S. Biniak, G. Szymanski, J. Siedlewski, A. Swiatkowski, Carbon 35 (1997) 1799–1810.
[49] Z.R. Yue, W. Jiang, L. Wang, S.D. Gardner, C.U. Pittman, Carbon 37 (1999) 1785–1796.
[50] M. Besson, P. Gallezot, Catal. Today 81 (2003) 547–559.
[51] J. Panpranot, O. Tangjitwattakorn, P. Praserthdam, J.G. Goodwin Jr., Appl. Catal. A: Gen. 292 (2005) 322–327.
[52] J.G. Ulan, W.F. Maier, J. Mol. Catal. 54 (1989) 243–261.
[53] G. Johansson, J. Hedman, A. Berndtsson, M. Klasson, R. Nilsson, J. Electron Spectrosc. Relat. Phenom. 2 (1973) 295–317.
[54] T.H. Fleisch, G.J. Mains, J. Phys. Chem. 90 (1986) 5317–5320.
[55] V.I. Nefedov, I.A. Zakharov, Moiseev II, M.A. Poraikos, M.N. Vargafti, A.P. Belov, Zh. Neorg. Khim. 18 (1973) 3264–3268.
[56] V.I. Nefedov, Y.V. Salyn, Moiseev II, A.P. Sadovskii, A.S. Berenbljum, A.G. Knizhnik, S.L. Mund, Inorg. Chim. Acta 35 (1979) L343–L344.